Ocean Dynamics (2016) 66:623–636
DOI 10.1007/s10236-016-0942-2

What dominates sea level at the coast: a case study for the Gulf of Guinea

Angélique Melet[1,2] · Rafael Almar[1] · Benoit Meyssignac[1]

Received: 1 June 2015 / Accepted: 24 February 2016 / Published online: 18 March 2016

Abstract Sea level variations and extreme events are a major threat for coastal zones. This threat is expected to worsen with time because low-lying coastal areas are expected to become more vulnerable to flooding and land loss as sea level rises in response to climate change. Sea level variations in the coastal ocean result from a combination of different processes that act at different spatial and temporal scales. In this study, the relative importance of processes causing coastal sea level variability at different time-scales is evaluated. Contributions from the altimetry-derived sea-level (including the sea level rise due to the ocean warming and land ice loss in response to climate change), dynamical atmospheric forcing induced sea level (surges), wave-induced run-up and set-up, and astronomical tides are estimated from observational datasets and reanalyses. As these processes impact the coast differently, evaluating their importance is essential for assessment of the local coastline vulnerability. A case study is developed in the Gulf of Guinea over the 1993–2012 period. The leading contributors to sea level variability off Cotonou differ depending on the time-scales considered. The trend is largely dominated by processes included in altimetric data and to a lesser extent by swell-waves run-up. The latter dominates interannual variations. Swell-waves run-up and tides dominate subannual variability. Extreme events are due to the conjunction of high tides and large swell run-up, exhibiting a clear seasonal cycle with more events in boreal summer and a trend mostly related to the trend in altimetric-derived sea-level.

Keywords Sea level · Altimetry · Waves · Coastal · Climate variability · Extreme events

Responsible Editor: Birgit Andrea Klein

✉ Angélique Melet
angelique.melet@legos.obs-mip.fr

[1] LEGOS, Université de Toulouse, CNES, CNRS, IRD, UPS, Toulouse, France

[2] Mercator-Ocean, Ramonville St. Agne, France

1 Introduction

Coastal regions are expected to increasingly experience severe impacts as sea level rises in response to climate change (Wong et al. 2013). These impacts include permanent submergence, more frequent coastal flooding during storm surges, accelerated erosion of coastlines, and salt intrusion in aquifers and surface waters (e.g., Nicholls and Cazenave 2010; Ranasinghe et al. 2012).

Sea level variations in the coastal ocean result from multiscales processes, with the superimposition of global, regional, and more local variations due to the combination of different processes. The leading contributors to contemporary global mean sea level rise are the thermal expansion of the warming ocean and the transfer of water mass from land (including glaciers, Greenland and Antarctic icesheets, icecaps, and groundwater) to the ocean (Church et al. 2013; Le Cozannet and Cazenave 2014). On top of global mean sea level rise, substantial regional variations in sea level result from heat, salt, and mass redistribution by the ocean circulation in response to atmospheric forcing (essentially winds but also heat and freshwater fluxes) (e.g., Timmermann et al. 2010; Stammer et al. 2013) and from atmospheric pressure loading variations at the sea surface (e.g., Wunsch and Stammer 1997). In addition, astronomical tides and waves produce sea level variations with an increasing amplitude over shallower regions such as the coastal zone. In the coastal band, a series of local processes also lead to sea level variations. Regional surface wind stress changes and related displacement of surface water induce a set-up (Walton and Dean 2009). Together with the ocean response to atmospheric wind and pressure forcing anomalies caused by atmospheric depressions, they induce storm surges that also impact coastal sea level. Finally, changes in locally generated wave (wind-wave) or remotely generated wave (swell) regimes can make significant contributions to coastal sea level changes through wave set-up (time-mean dynamic elevation of sea-level due to wave breaking) and run-up (waterline oscillations at the time scale of individual waves and wave groups) (Komar 1998; Stive 2004; Stockdon et al. 2006). Wave set-up and run-up can significantly contribute to extreme sea level events (Hoeke et al. 2013). At interannual to multi-decadal time-scales, these coastal processes have been poorly observed and it is not clear whether changes in wave run-up and set-up could significantly contribute to long-term coastal sea-level variations.

All the aforementioned processes co-exist and cause sea level to vary at the coast on a wide range of temporal and spatial scales, from short-lived events to sustained changes over several decades or centuries (e.g., Meyssignac and Cazenave 2012). It is essential to identify which ones dominate coastal sea level variations locally when assessing the vulnerability of the coast line. However, as of now, no observational system has measured all these processes simultaneously over long periods.

Tide gauges have measured sea level at the coast for decades (Mitchum et al. 2010). They have provided the primary data source for numerous analysis of sea level trends (e.g., Holgate 2007; Jevrejeva et al. 2008; Woppelmann et al. 2009; Ray and Douglas 2011; Church and White 2011; Meyssignac et al. 2012; Dean and Houston 2013; Becker et al. 2014) and of extreme events (e.g., Menendez and Woodworth 2010; Losada et al. 2013; Goddard et al. 2015). However, because of their location in the ocean and often in sheltered places such as harbors, tide gauges do not capture sea level variations due to waves run-up and could partly miss the contribution of wave set-up as the latter is induced by wave-breaking and increases from the breaking point to the coast. Therefore, tide gauges might not provide adequate data in wave-exposed areas.

Satellite altimetry has provided a powerful tool for studying sea level variations over the open ocean for more than 20 years. Altimeters measure sea surface height and its variations, without differentiating the various processes leading to those variations. Yet, as the primary focus of satellite altimetry is to study ocean circulation and dynamics, the contribution to sea-level variations due to the geoid, tides, and high-frequency wind forcing and atmospheric pressure loading are subtracted from the observed altimetric sea level. As waves influence altimetric measurements, a sea-state bias correction is also applied to altimetric data to remove this effect. The averaging of sea surface height over the altimeter footprint of a few kilometers also filters sea-level variations due to waves. So far, satellite altimeters have unfortunately performed satisfactorily only over the open ocean. In the coastal ocean, a number of issues arise due to both poorer geophysical corrections and to the vicinity of land, which influences the measurement of sea surface height with the altimeter. Therefore, altimetric data need to be improved in a coastal strip of a few tens of kilometers to be used to study coastal ocean dynamics (Birol et al. 2010; Vignudelli et al. 2011; Passaro et al. 2014).

Until recently, observations of wave-induced run-up and set-up were limited to short duration (from days to weeks, through intensive in situ measurements) or rather long-term low temporal resolution (monthly/yearly surveys through images from optical satellites or in-situ measurements).

The open ocean and littoral sea level research communities have therefore worked with different tools and techniques, as the dominant physical processes and spatio-temporal scales they are studying are different. Historically, this has limited exchanges between the two communities and most studies of sea level trends and extreme events at the coast do not take into account the contributions of all the different aforementioned drivers of coastal sea-level variations. Yet, significant progresses were made over the last years in estimating the sea level from altimetry-derived observations, wind and pressure forcing, wave-induced run-up and set-up, and astronomical tides. These progresses make it now possible to link the open-ocean and littoral sea level research communities and to combine the different components of total sea level in the coastal ocean to evaluate their relative contribution to sea-level changes.

The objective of the present study is to estimate from observations and reanalyses the relative contribution of all oceanic processes to the local coastal sea-level trend, interannual and sub-annual variabilities, and extreme events including the contributions from tides, altimetry-derived sea level, swell-waves and wind-waves set-up and run-up, wind set-up, and wind and atmospheric pressure forcing.

In this paper, we develop a case study at Cotonou (6.37° N, 2.42° E), located on the coast line of Benin in the Gulf of Guinea (Fig. 1). Cotonou is one of the largest West African city, and is particularly vulnerable to sea level rise impacts because of its location on a low-lying sand barrier and its low adaptation ability (Dasgupta et al. 2009).

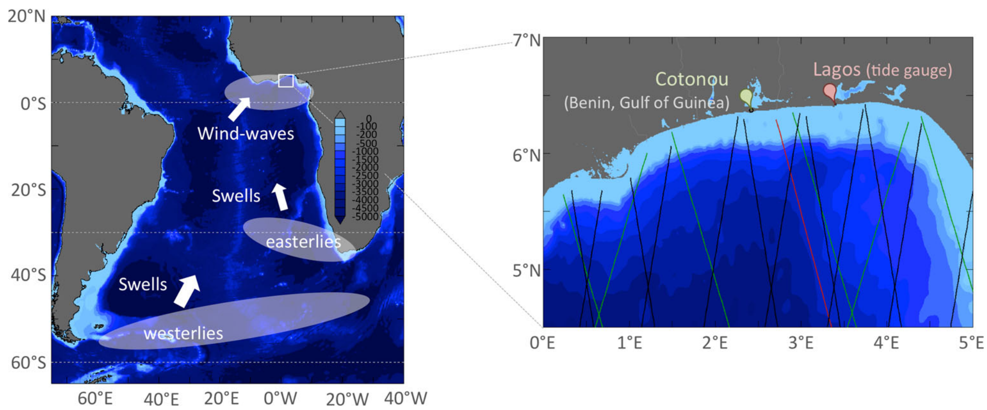

Fig. 1 (*Left*) Bathymetry (in meters, colorbar on the right) of the Atlantic and Southern oceans (from 75° E to 40° W and 65° S to 20° N). The regions of major generation of swells and wind-waves impinging on the Gulf of Guinea are indicated by the *white ovals*, and their major direction of propagation by the *white arrows*. (*Right*) Zoom on the Gulf of Guinea region offshore Cotonou, Benin. The *colorbar* is the same as for the left panel. Cotonou is located by the *green pin*, the Lagos tide gauge by the *red pin*. The tracks of the satellite missions merged in the AVISO gridded product used for the altimetric sea level are indicated: in *red* for Topex/Poseidon, Jason-1, and Jason-2; in *green* for GFO; and in *black* for ERS-1, ERS-2, and Envisat

2 Method and data

Total coastal sea level is calculated over the 1993–2012 period as:

$$SL = ASL + WW\_S + SW\_S + WW\_R + SW\_R + W\_S + AT + DA, \quad (1)$$

where ASL is the altimetry-derived sea level, WW_S is the wind-wave set-up, SW_S is the swell-wave set-up, WW_R is the wind-wave run-up, SW_R is the swell-wave run-up, W_S is the wind set-up, AT is the astronomical tide, and DA the sea level anomalies due to atmospheric wind and pressure forcing anomalies. Wind-waves are defined as waves with a period smaller than 8 s, and swell-waves by waves with a period greater than 8 s. Anomalies from the 1993–2012 mean are used.

The satellite altimetry data are extracted from the SSALTO/DUACS multimission gridded and delayed-time product (version 2014). In this product, the along-track data of Topex/Poseidon, Jason-1, Jason-2, GFO, ERS-1, ERS-2, Envisat, and Cryosat-2 (Fig. 1) are merged and mapped onto a 1/4° grid. The temporal resolution of the altimetric product is daily, although the satellite data are provided at a lower time resolution: Topex-Poseidon, Jason-1, and Jason-2 share the same ground tracks, with a repeat cycle of 9.916 days; GFO had a 17 days repeat cycle; ERS1, ERS2, and ENVISAT shared the same ground tracks and had a 35 days repeat cycle. We extracted altimetric sea level anomalies at the grid point closest to Cotonou, which is located at 2.375° E and 6.375° N.

The astronomical tide sea level elevations are provided by the global tide model finite element solution (FES) 2014 (see Carrère et al. (2012) for a description of the FES tidal model). AT is computed every hour at the grid point closest to Cotonou (2.42° E and 6.35° N) using the 32 major tidal constituents.

The pressure and wind meteorological forcing induced sea level (corresponding to the geophysical dynamic atmospheric correction applied to altimetric data) is provided by the Mog2D-G High Resolution (1/4°) barotropic model (Carrère and Lyard 2003; Carrère et al. 2012) forced by the pressure fields provided by the European Centre for Medium-range Weather Forecasting (ECMWF) reanalysis ERA-Interim for high-frequency variations (i.e., less than 20 days). At lower frequencies (i.e., more than 20 days), an inverted barometer correction (Wunsch and Stammer 1997) is applied, assuming a static response of the ocean to atmospheric forcing, and neglecting wind effects. The combined high-frequency and low-frequency dynamic atmospheric forcing induced sea level is calculated every 6 h at the ocean grid point closest to Cotonou (2.5° E and 6.25° N).

The wind-induced set-up is included in the dynamic atmospheric forcing induced sea level. However, the model we used (Mog2D-G) has a resolution of 1/4°, which is not sufficient to realistically reproduce the wind-induced set-up at the coast which essentially depends on the shelf depth and width. The continental shelf offshore Cotonou is narrow (∼30 km, Fig. 1). Therefore, we estimated the coastal wind-induced set-up (W_S) daily using the ECMWF ERA-Interim wind hindcast (Dee et al. 2011) and the formulation proposed by Walton and Dean (2009):

$$x/L = \left(1 - \frac{h + W\_S}{h_0}\right) - A \ln\left(\frac{(h + W\_S)/h_0 - A}{1 - A}\right), \quad (2)$$

where x is the distance from the continental shelf (positive towards the coast), L is the shelf width, h is the water depth,

h_0 is the depth of water at the seaward edge of the shelf, and A is on non-dimensional coefficient given by:

$$A = \frac{1.15\tau_{wx}L}{\rho g h_0^2}, \tag{3}$$

where ρ is the density of sea water and τ_{wx} is the cross-shore component of the wind stress.

Wave-induced set-up is estimated using the parameterization of Stockdon et al. (2006) and is a function of the deepwater wave steepness (ratio of the wave height over the horizontal wavelength) and of the beach slope:

$$\eta = 0.45 H_0 \epsilon_0, \tag{4}$$

where η is the wind-wave or swell-wave induced set-up (WW_S and SW_S, respectively, depending on the period of the waves) and H_0 is the deep water wave height. ϵ_0 is the non-dimensional surf-similarity parameter (Battjes 1974) defined as:

$$\epsilon_0 = tan\left(\frac{\beta}{\sqrt{H_0/L_0}}\right), \tag{5}$$

with β the nearshore topographic slope, taken here as the observed mean value of 0.15 (Almar et al. 2015), and L_0 the wavelength of the waves in deep water. Waves induced set-up are estimated every 6 h based on the ECMWF ERA-Interim wave hindcast (Dee et al. 2011) for H_0 and L_0.

After breaking, in the surf zone, non-linear wave-energy transfers toward different frequencies occur so that both swells and wind-waves can feed the infra-gravity band (period greater than 20 s) (Longuet-Higgins and Stewart 1962). The set-up and set-down rising from the time-varying breakpoint of the grouped short waves also forces infra-gravity waves (Symonds et al. 1982). Wave-induced run-up is estimated using the parameterization of Holman and Sallenger (1985):

$$R = \kappa_{osc}\frac{\sqrt{R_{ig}^2 + R_{ic}^2}}{2}, \tag{6}$$

where R_{ig} and R_{ic} are the run-up due to infra-gravity swell waves and swash incoming waves (period shorter than 20 s) respectively, and κ_{osc} is a constant, non-site-dependent empirical coefficient that accounts for the level of swash exceedence. κ_{osc} is taken to 1.37 here (see Stockdon and Holman 2000) computed separately for oscillations at incident R_{ic} and infra-gravity R_{ig} frequencies. Holman and Sallenger (1985) found linear relationships between the normalized infra-gravity swash height R_{ig}/H_0 and the normalized sea swell swash height R_{ic}/H_0 to the surf-similarity parameter ϵ_0 following:

$$R_{ig} = H_0\,(0.53\epsilon_0 + 0.09)\,. \tag{7}$$

$$R_{ic} = H_0\,(0.69\epsilon_0 - 0.19)\,. \tag{8}$$

The relative contribution of R_{ic} and R_{ig} depends both on the slope of the beach and on offshore wave conditions: R_{ic} is dominant at steep beaches and R_{ig} at gentle slope beach where the surf zone is wide and saturated (Ruessink 1998). Wave run-up is estimated every 6 h based on the ECMWF ERA-Interim wave hindcast for H_0 and L_0.

3 Relative contributions of sea-level components

3.1 Trend, interannual, and subannual variabilities

Time-series of the different components of coastal sea-level variability at Cotonou are shown in Fig. 2. To evaluate the contribution of each component to coastal sea level trend, interannual and sub-annual variabilities at Cotonou, time series of each component are interpolated on the daily time sampling of altimetric data. The total coastal sea level, defined here as the sum of all components, is shown in Fig. 2 (dark blue line). Interactions between the different components are possible (for instance, non-linear tide-surge interactions can occur over wide and shallow shelves, Losada et al. (2013)) but are disregarded here.

The trend of each contributor is extracted through a linear regression and is listed in Table 1. To evaluate the significance of the trend relative to trends that could arise from random fluctuations over this 20-year period, a Monte Carlo test has been performed for each sea-level component (except for the tidal sea level, which is deterministic and oscillatory). We focused on trends induced by the 2- to 7-years interannual variability. 10^4 random time-series were generated using an auto-regressive model (AR) of order 2 to model the autocorrelation in the 2- to 7-year interannual variability (which is the classical approach for climate records in the tropics, see Von Storch and Zwiers (1999)). The random time-series have a variability that is similar to that of the detrended time-series of the sea-level component that is studied in terms of mean, variance, and power spectrum over the 2- to 7-year period. The distribution of the trends is then generated for each component and the 95 % confidence level for the significance of the trend corresponds to the percentile 0.95 of the cumulative distribution function. It should, however, be noted that long-term (decadal to muti-decadal) sea level variations due to natural variability could be significant (Dangendorf et al. 2014). The 95 % confidence level on the unforced trend in sea level provided in Table 1 (from 20-year time series and focusing on the 2- to 7-year variability) might therefore be underestimated. From this analysis, it is found that only the trend of ASL is significant at the 95 % confidence level (Table 1). The trends in other sea level components are indistinguishable form trends induced by random fluctuations at periods ranging from 2 to 7 years.

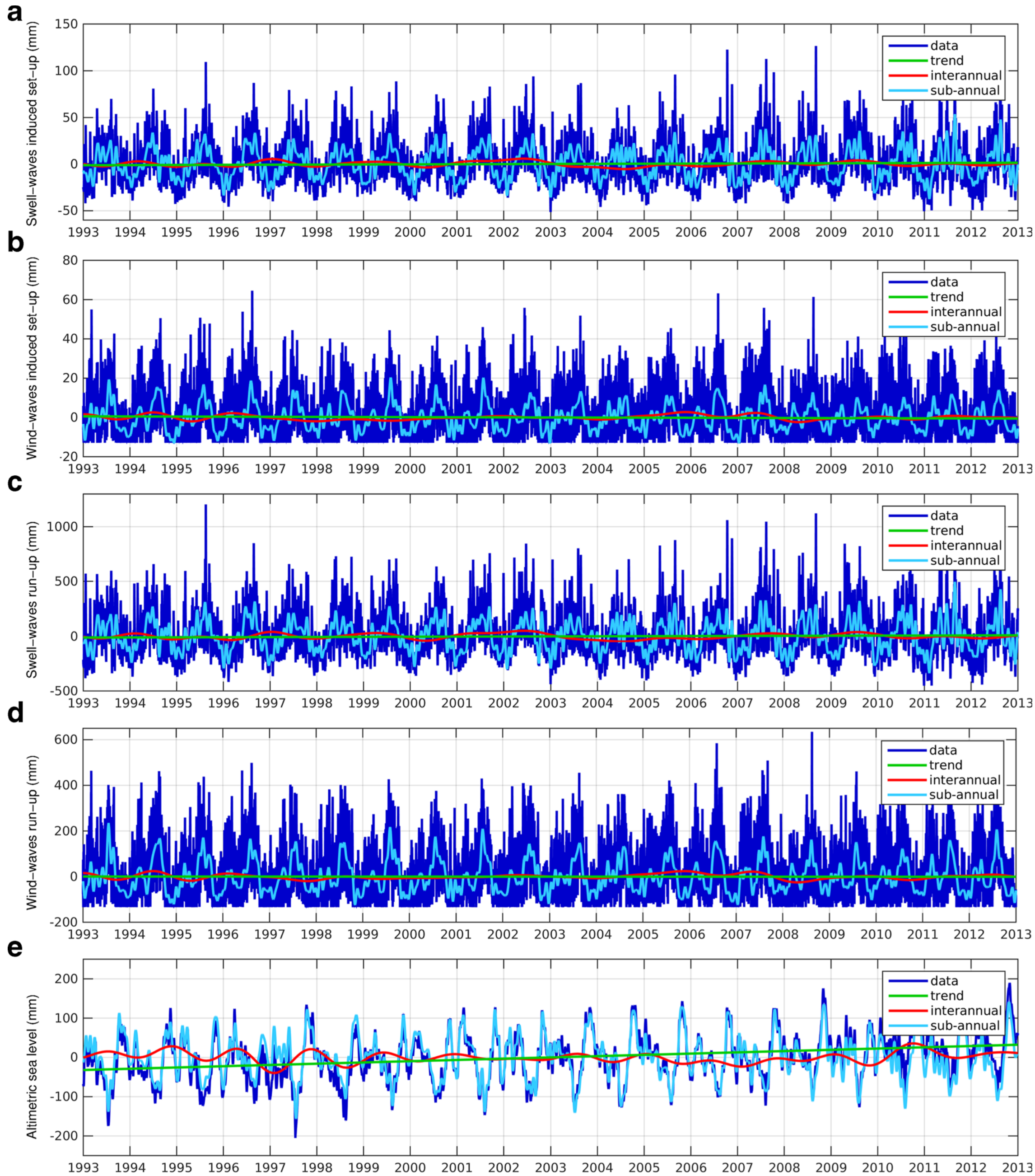

Fig. 2 Time-series of the different contributors to sea-level anomalies at Cotonou, Benin, for the 1993–2012 period relative to the 1993–2012 mean (in mm): **a** swell-waves induced set-up, **b** wind-waves induced set-up, **c** swell-waves run-up, **d** wind-waves run-up, **e** altimetric sea level, **f** dynamic atmospheric forcing (wind + pressure) induced sea level, **g** tidal sea level, **h** coastal wind-induced set-up, **i** sum of all contributors (**a** to **h**) at a daily resolution. In each panel, the time-series is shown in *dark blue*, the linear regression (trend) in *green*, the interannual variability of the detrended time-series in *red*, and the sub-annual variability of the detrended time-series in *light blue*

Interannual and subannual variabilities are computed from the detrended time-series. Interannual variability is extracted using a low-pass hamming filter with a cutoff frequency of 1.3 years. Subannual variability is extracted using a low-pass hamming filter with a cutoff frequency of 30 days and a high-pass hamming filter with a cutoff frequency of 1.3 years. The total sea level variability at subannual and interannual time scales are represented in Fig. 2a.

The contribution of each component to sea level trend, interannual and sub-annual variability are shown in Fig. 3a in terms of variance explained in the total coastal sea level. Clearly, the variance of the sea level at Cotonou is dominated by high-frequency variability (higher than monthly). Interannual variability and linear trend contribute two orders of magnitude less than subannual variability. However, the sum of sea level trends from each component leads to a trend

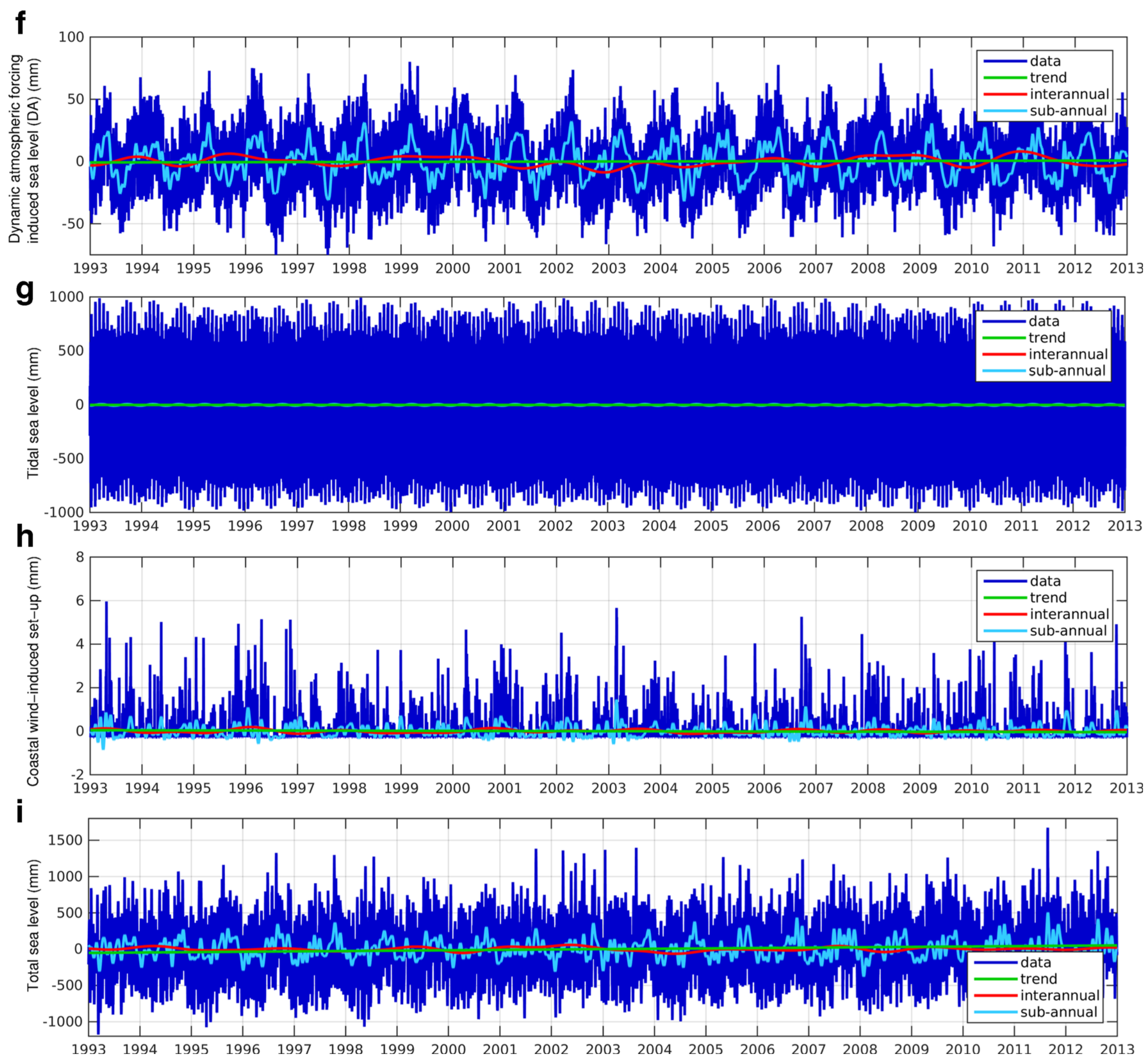

Fig. 2 (continued)

of 5.1 mm year^{-1}, therefore representing a rise of 13 cm over the 20-year period of this study.

To highlight the contribution of each component to the variance of sea level at the different time-scales considered here, Fig. 3b shows the percentage of the sum of the variances due to each component. By construction, the sum of the contributions equals 100 %. However, the sum of the variances does not necessarily equals the variance of the total sea level because different contributors are not totally independent and can vary partly either in or out of phase. Covariances between the different contributors were neglected here. Physically, we do not expect strong covariances between the different processes at long time-scales. The shortness of the observational time-series used here can, however, lead to covariances, especially between the interannual variability of the different variables.

When all time scales are considered, sea-level variance is mostly due to tides (72 %) and swell-waves run-up (20 %, Fig. 3b). Yet, tidal amplitudes are not especially high in the Gulf of Guinea (standard deviation of 397 mm in our dataset). The Gulf of Guinea is an open wave-dominated environment. Swell-waves impinging on the coast of Benin are generated by distant strong westerlies in the Atlantic sector of the Southern Ocean (45–60° S, Fig. 1) (Toualy et al. 2015; Almar et al. 2015, and references within). At Cotonou, swell-wave run-up is especially large due to the combination of weak dissipation on the narrow continental shelf, steepness of the beach, and extremely long-period swells. The contribution of swell-waves run-up also dominates the subannual (30 days to 1.3 years) variability (45 %) of the total sea level. The second largest contributor to subannual variability is tides (36 %), followed by wind-wave run-up (11 %) and altimetric sea level (8 %).

At interannual time-scales, sea-level variance is dominated by swell-waves run-up variability (61 %), with a smaller contribution from altimetric sea level (20 %) and

Table 1 (Left) Trends (in mm year^{-1}) of the different sea level components computed from a linear regression of the time-series over 1993–2012. (Middle column) Formal error in the trend related to the linear fit of the time-series are given in the "Uncertainty" column

Sea level component	Trend	Uncertainty	95 % CL trend
Swell-waves set-up	0.13	0.02	0.69
Wind-waves set-up	−0.06	0.01	0.31
Swell-waves run-up	1.05	0.20	5.98
Wind-waves run-up	−0.05	0.11	3.17
Altimetric sea level	3.21	0.12	2.64
Dynamic atmospheric forcing	0.07	0.02	5.81
Tides	−0.01	0.16	/
Wind set-up	−0.01	0.00	0.01
Extreme events	3.86	1.64	0.77

The 95 % confidence level (CL) for the significance of the trend is indicated in the right column. As tides are deterministic, no confidence level for the significance of the trend is provided. Trends in sea levels reached during the 2 % extreme-most events, their uncertainty, and 95 % confidence level of significance are listed in the last row

wind-wave run-up (16 %). At interannual time-scales, the height of swell waves generated in the Atlantic sector of the Southern Ocean is negatively correlated with the Southern Annular Mode (SAM) during austral winter (Hemer et al. 2010). In the Tropical Atlantic ocean, interannual sea level variability observed by altimetry is strikingly low compared to observed variability in the Tropical Indian and Pacific Oceans. The relatively high ASL interannual variability in the Indian and Pacific Oceans can be attributed to internal climate modes such as El Niño Southern Oscillation and their induced changes in the ocean circulations and thermal structure. By contrast, sea level interannual variability in the Tropical Atlantic is mainly driven by surface buoyancy forcing, and is therefore directly related to local atmospheric forcing (Chang et al. 2006; Cabanes et al. 2006; Piecuch and Ponte 2013).

The sea-level trend is mostly explained by the trend in altimetry-derived sea level (88 %). This trend is significantly (at a 95 % confidence level, Table 1) different from trends that could arise from the 2- to 7-year interannual variability. It arises partly from the low-frequency variability (below 7 years) and partly from the long-term sea level trend induced by climate change. Recent studies have indeed shown that as the Tropical Atlantic is a region of small internal variability, the climate change forced trend in sea level emerges the earliest from internal variability in this region (Lyu et al. 2014; Bilbao et al. 2015).

Unexpectedly, the swell-wave run-up contribution is not negligible and explains another 10 % of the sea-level trend. However, this trend is not significant at a 95 % confidence level (Table 1) and likely arises from the SAM-induced variability. The current positive trend in SAM is associated with a southward displacement of the storm track (Hemer et al. 2010), which induces a modification of swell-waves directions with an increasing amplitude in the cross-shore direction.

The coastal wind set-up (W_S) is small in the open Gulf of Guinea, which further exhibits a narrow continental shelf. As a result, the wind set-up contribution to total sea-level is negligible at all time-scales (Fig. 3).

3.2 Extreme events

Physical coastal impacts are most pronounced during episodes of extreme sea levels (Woodworth et al. 2004), which usually arise from the combination of the different sea level components considered in this study.

Extreme events are defined here as the highest 2 % of the total sea level time series (percentile 0.98 of the sea level distribution), computed as the sum of the time-series of each components interpolated to a 1-h resolution time axis. Only the extreme-most sea level per 3-day windows are selected so that only the highest sea levels caused by different consecutive events are considered, leading to a total of 345 extreme events over the 1993–2012 period (Fig. 4a).

Percentages of the total number of extreme events binned per year and per month are shown in Fig. 4b, c, together with the mean relative contribution of each sea level component. The number of extreme events shows a large interannual variability (from 9 events in 2004 to 23 events in 2002). At interannual time-scales, the leading contributor to extreme events is the swell-wave run-up, in conjunction with high tides and swell-wave set-up (Fig. 4a). The altimetric sea level is not a large contributor to sea level extreme events, but a positive trend of its contribution is shown in Fig. 4a. A trend of 3.86 mm year^{-1} is seen in the extreme sea levels over the 20-year period (Table 1). To assess the significance of the trend in the extreme sea levels reached during the

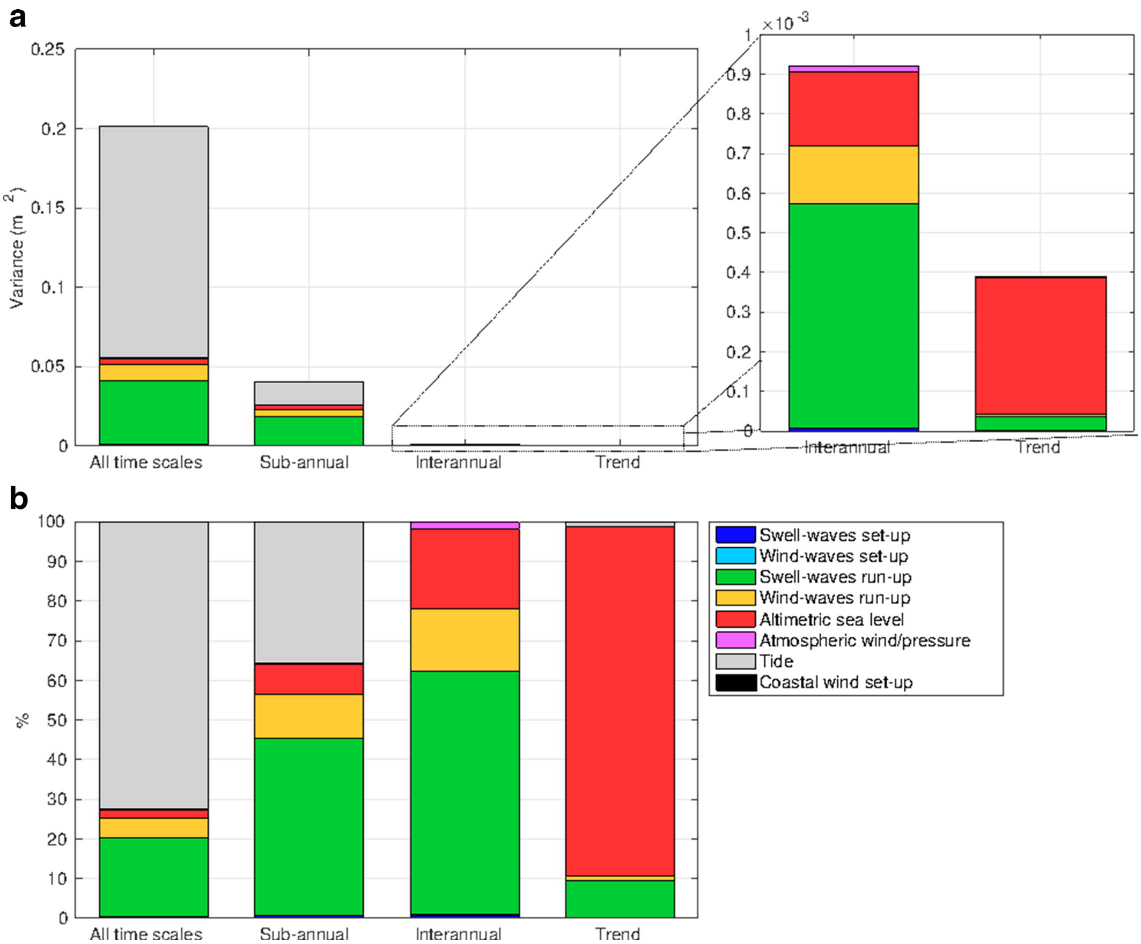

Fig. 3 **a** Variance (in m^2) of the different sea level components when all time-scales are considered, at sub-annual time-scales, interannual time-scales, and for the linear regression of the time-series. A zoom for the variances of interannual time-series and of linear regressions is provided on the right panel. **b** Contributions (in %) of the variance of the different sea level components to the sum of the variances of each component

345 analyzed events, a Monte Carlo test was performed. Although tides are deterministic, the 345 extreme events do not exhibit a deterministic tidal contribution. Therefore, the tidal contribution was not removed from the total sea level to assess the significance of the trend. 10^4 random time series with amplitudes corresponding to the standard deviations of the detrended extreme-sea-levels time-series were generated and their trend was computed. The distribution of the trends is then generated and the 95 % confidence level for the significance of the trend (corresponding to the percentile 0.95 of the cumulative distribution function) equals 0.77 mm year^{-1} (Table 1). The trend in extreme sea-levels over the 20-year period is therefore significant at the 95 % confidence level. Previous studies reported that trends in extreme sea-level are due to trends in mean sea level rather than to trends in weather patterns (e.g., Menendez and Woodworth, 2010; Losada et al. 2013). Our results support the fact that the trend in altimetric sea level (of 3.21 mm year^{-1} offshore Cotonou) dominates the trend in extreme events.

Extreme sea level events show a clear seasonal cycle, with more events in boreal summer and less events in boreal winter (Fig. 4b). This seasonal cycle is mostly related to the annual cycles of swell-wave and wind-wave run-ups, which are maximum in boreal summer. Swell waves reaching the Gulf of Guinea are dominated by swells generated in the Atlantic sector of the Southern Ocean (Fig. 1). These swells are more energetic in austral winter (boreal summer), when the wind forcing is stronger in the Southern Ocean. The trade winds in the eastern tropical Atlantic are also stronger in boreal summer, when the Intertropical Convergence Zone (ITCZ) is at its northernmost latitude, generating more energetic wind waves (Richter et al. 2014). Set-up and run-up due to wind-waves and swells have the same seasonal cycle,

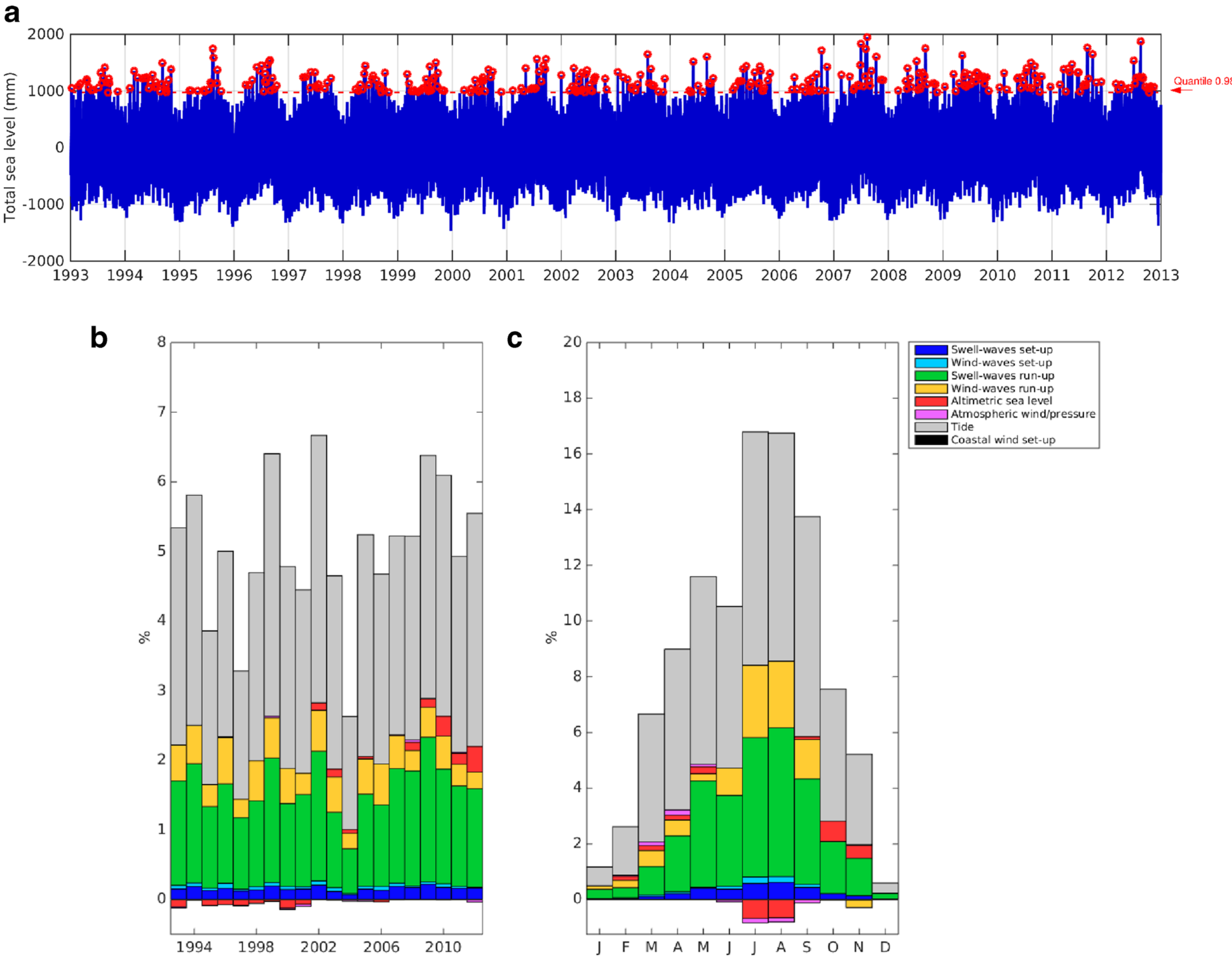

Fig. 4 **a** The time-series of total sea level anomalies relative to the 1993–2012 mean (sum of all contributions interpolated on a 1-h resolution time-axis) is shown in *dark blue*. The percentile 0.98 of the sea level defining the 2 % highest sea levels is indicated by the *red dashed line* and *red arrow*. The corresponding extreme events are indicated by *red dots*. Only the extreme-most sea level is considered per 3-day windows. **b** Number of extreme events per year and **c** per month (shown in percentage, for a total of 345 extreme events). For each bar, the mean contribution of each sea level component to the total sea level is shown using the same color code as in Fig. 3

but run-up has larger amplitudes than set-up and therefore contributes more to extreme events. Tides are the second contributor to extreme events at seasonal time-scales, as they were at interannual time-scales. ASL does not contribute much to the seasonality of extreme events. Wind stress curl variations due to the annual march of the ITCZ and the induced vertical advection associated with local Ekman pumping are the leading mechanisms for the seasonal cycle of the Gulf of Guinea ASL (Vinogradov et al. 2008), which is maximum in boreal spring and minimum in boreal fall. The ASL seasonal cycle therefore tends to slightly offset the amplitude of extreme events.

Note that results are robust to the choice of the quantile used to select extreme events.

4 Comparison to tide gauge data

The closest tide gauge to Cotonou with available data is located at Lagos (Nigeria), roughly 100 km away from Cotonou (Fig. 1). The tide gauge record is incomplete, covering only years 1993 to 1996 with major data gaps. No GPS data is available to account for vertical motions of the land. The following comparison of our results to the Lagos tide gauge data is therefore mostly qualitative. Figure 5 shows the Lagos hourly tide gauge data over 1993–1996, the hourly time-series of the sum of all contributors to sea level (total sea-level) variations at Cotonou, of the total sea-level without the contribution of wind-waves and swell-waves run-up and set-up and of tides. Clearly, sea level variations are larger in the total sea level than in the tide gauge data (Fig. 5a). This is largely due to the fact that swell-waves and wind-waves induced set-up and run-up are hardly captured by the tide gauge. When these contributions are removed from the total sea level, a better agreement is found with the tide gauge data (Fig. 5b–d). The fact that swell-waves and wind-waves induced set-up and run-up are hardly captured by the tide gauge is further supported when looking at a shorter time-period. The most devastating storm surge of the 1985–1995 period in Lagos was documented to occur on the 17th of August, 1995. This event resulted in a 5- to 8-m erosion of the beach. This event is one of the 345 extreme

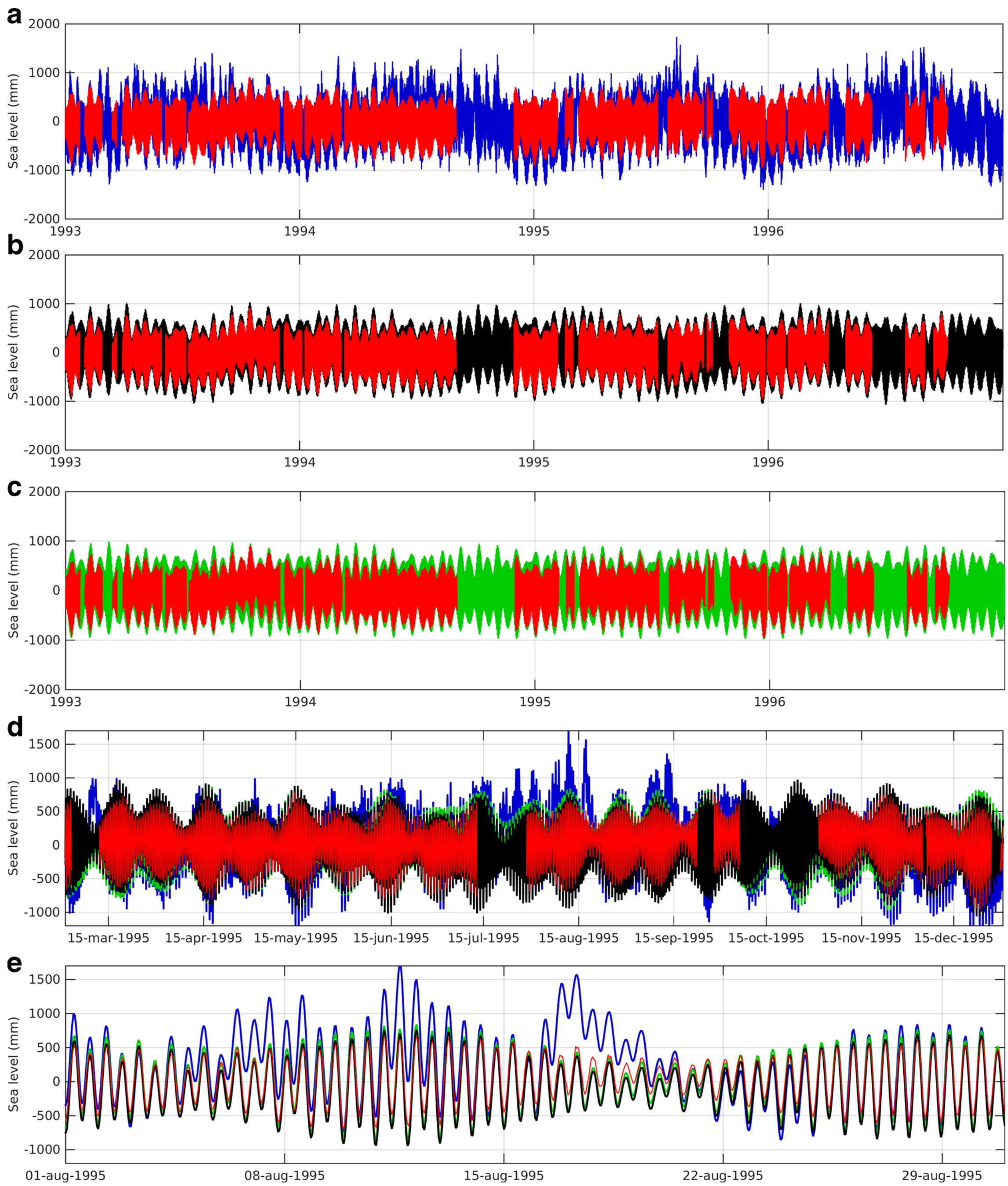

Fig. 5 Comparison to tide gauge data. Time-series of **a** the sum of contributors to sea-level variations at Cotonou (in *blue*, ASL + WW_S + SW_S + WW_R + SW_R + W_S + AT + DA), **b** the sum of contributors to sea-level variations at Cotonou but excluding the wind-waves and swell-waves induced run-up and set-up (in *black*, ASL + W_S + AT + DA), and **c** the tides (in *green*). In panels (**a**) to (**c**), the Lagos (Nigeria, see Fig. 1) tide gauge data is shown in *red*. Zooms of the different time-series over **d** the 15-march-1995 to 15-dec-1995 period and **e** the month of August 1995 are also shown, using the same color code as in panels (**a**) to (**c**)

events analyzed in our study. Figure 5d shows that this extreme event occurred during neap tides, and was indeed mostly due to waves run-up and set-up (compare the blue, black, and red lines). In the total sea level time series calculated in this study, the highest sea level during August 1995 occurs on the 12th, a week before the documented event of August 17th. Different sources of errors or uncertainties can account for this, including uncertainties in wave data, neglecting interactions between the different contributors of sea level variations, the fact that the tide gauge data is for Lagos while our total sea level time series is calculated off Cotonou. Finally, sediment transports and changes in the seabed topography are not accounted for in this study. The beach response to a storm depends on the recent history of storm events, as the beach and seabed topography are modified for several days after a storm (Coco et al. 2014). The event that occurred on August 12th, 1995 (itself preceded by an event on August 8th, 1995) could have modified the sea bed topography, leading to a more damaging event a few days later on August 17th, 1995 when the sea level reached again extreme levels.

5 Conclusion and discussion

The contributions of the different drivers of coastal sea-level variations and rise are assessed for Cotonou (Benin, Gulf of Guinea) over 1993–2012 using existing observational datasets and reanalysis for each contributor. The objective is to provide an estimate of the importance of the different processes causing sea level variations at different time-scales in order to identify the locally relevant climate and oceanic processes against which protection could be planned.

Our diagnostics show that the leading contributors to sea level variability differ depending on the time-scales considered. Extreme events of high sea levels are due to the conjunction of high tides and large swells run-up. Extreme events exhibit a clear seasonal cycle with more events in July–August, which is caused by the seasonal cycle of swells run-up as swells impinging on the Gulf of Guinea mostly originate from the Southern Ocean, where winds are stronger in austral winter. Subannual variability is dominated by swell-waves run-up and tides. Interannual sea-level variability is dominated by swell-waves run-up. Sea level trend is largely dominated by the trend in altimetry-derived sea level, which captures the trend in sea level notably due to the ocean water expansion induced by ocean warming, changes in ocean circulation, and the increase of the ocean mass due to land-ice loss. However, we note that swell-waves run-up plays a significant role over the last 20 years. This result suggests that at decadal to multidecadal (and potentially longer) time scales, run-up changes, from swell-waves in particular, can play a role on coastal sea level trends and should be taken into account in long term impact studies.

While contributors to sea level changes captured in altimetric data only weakly contribute to extreme events at Cotonou over the 20-year period studied here, they account for most of the sea-level trend over that period. The rise in sea level due to a warming ocean and loss of land-ice mass is projected to accelerate during the 21st century (Church et al. 2013) and is only limited by the amount of land ice that will be transferred to the ocean and the amount of climate change related excess heat that will be stored in the ocean. Moreover, the sea level rise captured by altimetry aggravates extreme events due to the conjunction of swells and waves set-up and run-up, wind set-up, atmospheric loading, and tides. Therefore, the contribution of altimetric sea level to extreme events and sea-level rise is expected to increase significantly in the future, whereas the amplitude of sea-level variability due to tides, wind set-up, waves, and atmospheric loading are not expected to change as dramatically over the next century. Projections of changes in wave climate remain largely uncertain under the twenty-first century (Church et al. 2013). The Southern Ocean is projected to experience the largest changes in significant wave height (Hemer et al. 2013), with an increase by 5 to 10 % at the end of the twenty-first century compared to the present-day mean. This projected increase in significant wave height in the Southern Ocean reflects the projected strengthening of the westerlies in that region, particularly during austral winter (Church et al. 2013). Consistent with a higher contribution from the northward propagating swell generated in the Southern Ocean, wave direction is projected to rotate clockwise in the tropics, and wave period is projected to slightly increase in the Gulf of Guinea (Hemer et al. 2013).

Our results are subject to different sources of uncertainties. First, interactions and correlations between the different components of coastal sea-level variability were disregarded in this study, which focuses on a region with a narrow shelf. Yet, interactions between the mean sea level, waves, tides, and atmospheric surges (caused by changes in atmospheric winds and pressure) exist. Such interactions are caused by several mechanisms, and become more important for regions with wide continental shelf (e.g., Wolf (2009) and references within, Bertin et al. (2012)). For instance, as wave height in the coastal ocean is largely controlled by water depth, it can be modulated by tides and impacted by changes in sea level in the coastal ocean due to atmospheric surges or dynamic ocean processes and climate change. As the water depth changes in the coastal ocean, the loss of energy by tides and waves due to bottom friction also changes. Wave-induced set-up and run-up are also impacted by changes in bathymetric slopes in the surf zone inferred by changes in water depth. Waves may affect the generation of atmospheric surges by affecting the sea surface roughness and momentum transferred from the wind to the ocean surface flows. Since interactions between the different drivers of sea-level variability in the coastal ocean might be non-negligible, especially for regions with a wide continental shelf, but are not yet completely well understood, further investigation are needed to better take them into account. As a result of non-linear interactions between offshore mean sea level, tides, and dynamic atmospheric forcing induced sea level changes, changes in extreme events under climate change can therefore deviate from increases in mean sea level (Arns et al. 2015).

Secondly, datasets used in this study have uncertainties. The uncertainty in local altimetric measures at 1 Hz is of 1–2 cm, and of 1.5 mm year^{-1} for the 20-year sea-level trend near Cotonou (P. Prandi, personnal communication). Higher quality satellite altimetry data in the coastal zone such as the data currently collected by SARAL/AltiKa and the data that will be collected by the SWOT mission will improve our understanding and estimate of contributors to coastal sea-level variations. Yet, the highest uncertainties currently lie in the contributions of coastal processes such as wind set-up, waves set-up and run-up, and of the inverted barometer effect. Even though these processes are crucial for coastal erosion and submersion and despite recent progresses, large uncertainties remain on the estimates of their contribution to total sea level (Stockdon et al. 2006). Set-up and run-up estimates have generally uncertainties in the order of O(10 cm) at daily time-scales, about 10 % of the offshore wave height (Stockdon et al. 2006; Aarninkhof et al. 2003; Serafin and Ruggiero 2014). Direct observations of wave-induced runup and setup are scarce, and quantifying prediction errors is a difficult task (Stockdon et al. 2006; Laudier et al. 2011; Plant and Stockdon 2015). Several studies (e.g., Guza and Feddersen, 2012; Matias et al. 2012; Senechal et al. 2011) suggest that discrepancies between parameterized and observed waterline levels can be attributed to a number of factors, including uncertainties in nearshore wave height, in wave-directional spectra (Guza and Feddersen 2012), in the spatio-temporal variability of the beach topography, and in wave breaking variations related to different tide levels (Guedes et al. 2011). In particular, run-up and set-up might substantially vary over a tidal cycle at intermediate low-tide terrace beaches (Wright and Short 1984) as encountered in the Bight of Benin (Laibi et al. 2014; Almar et al. 2015) which present a flat lower part and a steep upper part. Separating the causes of uncertainties is challenging and would require a dataset that resolves each of the contributing processes (Plant and Stockdon 2015). Using coastal video observations (Almar et al. 2014) and field measurements in the Bight of Benin, Abessolo et al. (submitted) observed a substantial variation of the beach slope at event (i.e., storms) and seasonal scales.

Our results further advocate a need for a strong research effort to better observe and understand nearshore processes components and their variability along different types of coastlines, particularly at long time-scales. The emergence of video monitoring systems could provide observations of the near-shore sea-level variability including the contribution of wave-induced run-up and set-up. Over time, such observations could also be useful to test and validate the methodology used in the present study.

Finally, assessments of coastal sea level impacts need to consider sea level relative to the position of the coast, hence changes in the position of the coastline and vertical land motions. A variety of local processes unrelated to the ocean variability but impacting relative sea level are not taken into account in this study. At large scales, vertical land motion is caused by the long-term glacial isostatic adjustment of the solid Earth to the last deglaciation (e.g., Tamisiea 2011). More local land subsidence or uplift can be caused by sediment compaction and loading and by tectonics.

While this paper focused on Cotonou, Benin, the same methodology could be applied in future studies on contrasted coastal sites worldwide as the importance of the different drivers of coastal sea level variability are expected to largely vary for different coastal locations (e.g., Losada et al. 2013). Over 1993–2012, sea level rise at Cotonou from altimetric data is close to the global mean sea level rise (of 3.1 mm/year, e.g., Church et al. (2013)), but regions such as the tropical western Pacific have experienced rates of rise three times larger (e.g., Meyssignac et al. 2012; Merrifield et al. 2012; Hamlington et al. 2014; Palanisamy et al. 2015). The Gulf of Guinea is an open wave-dominated environment. Swell-waves originating from the Atlantic sector of the Southern Ocean and impinging on the Gulf of Guinea are energetic and present long periods. As they are modulated by the Southern Annular Mode, the contribution of swell-waves run-up to sea level variability is large at interannual time-scales at Cotonou. However, the contribution of swell-waves run-up is expected to largely vary across different coastal sites. As the continental shelf is narrow offshore Cotonou, the sea level set-up due to the wind stress and to the breaking of wind-waves and swell-waves is limited. However, the contribution of these sea-level components is expected to be larger for coastal sites located in regions with large continental shelves. Finally, the tidal regime is microtidal (from 0.3 to 1.8 m for neap and spring tidal ranges, respectively). Tides are expected to contribute more largely to subannual variability in other coastal sites located on macro-tidal coasts.

Acknowledgments The altimeter products were produced by Ssalto/Duacs. The altimeter products and the dynamic atmospheric corrections are distributed by AVISO, with support from CNES (http://www.aviso.altimetry.fr/). Dynamic atmospheric corrections are produced by CLS Space Oceanography Division using the Mog2D model from LEGOS. The authors thank Florent Lyard for providing the tidal predictions off Cotonou of FES2014. Tide gauge data were downloaded from the University of Hawaii Sea Level Center (http://uhslc.soest.hawaii.edu).

References

Aarninkhof SGJ, Turner IL, Dronkers TDT, Caljouw M, Nipius L (2003) A video-based technique for mapping intertidal beach bathymetry. Coast Eng 49(4):275–289

Almar R, Du Penhoat Y, Honkonnou N, Castelle B, Laibi R, Anthony E, Senechal N, Degbe G, Chuchla R, Sohou Z, Dorel M (2014) The Grand Popo experiment, Benin. J Coast Res Spec Issue 70:651–656

Almar R, Kestenare E, Reyns J, Jouanno J, Anthony E, Laibi R, Hemer M, DuPenhoat Y, Ranasinghe R (2015) Response of the Gulf of Guinea coastline to anthropogenic and natural forcing, Part1: wave climate variability and impacts on longshore sediment transport. Continental Shelf Research in press, doi:10.1016/j.csr.2015.09.020

Arns A, Wahl T, Dangendorf S, Jensen J (2015) The impact of sea level rise on storm surge water levels in the northern part of the German Bight. Coast Eng 96:118–131

Battjes J (1974) Surf similarity. In: Proceedings of the 14th Conference of Coastal Engineering. ASCE

Becker M, Karpytchev M, Lennartz-Sassinek S (2014) Long-term sea level trends: natural or anthropogenic? Geophys Res Lett 41:5571–5580

Bertin X, Bruneau N, Breilh J, Fortunato A, Karpytchev M (2012) Importance of wave age and resonance in storm surges: the case Xynthia, Bay of Biscay. Ocean Model 42:16–30

Bilbao RA, Gregory JM, Bouttes N (2015) Analysis of the regional pattern of sea level change due to ocean dynamics and density change for 1993–2099 in observations and CMIP5 AOGCMs. Clim Dyn 45(9):2647–2666

Birol F, Cancet M, Estournel C (2010) Aspects of the seasonal variability of the Northern Current (NW Mediterranean Sea) observed by altimetry. J Mar Syst 81:297–311

Cabanes C, Huck T, Colin de Verdire A (2006) Contributions of wind forcing and surface heating to interannual sea level variations in the Atlantic Ocean. J Phys Oceanogr 36:1739–1750

Carrère L, Lyard F (2003) Modelling the barotropic response of the global ocean to atmospheric wind and pressure forcing—comparisons with observations. Geophys Res Lett 30(6):1275

Carrère L, Lyard F, Cancet M, Guillot A, Roblou L (2012) FES2012: A new global tidal model taking advantage of nearly 20-years of altimetry. In: Proceedings of the 20 Years of Progress in Radar Altimetry Symposium, Venice, Italy

Chang P, Yamagata T, Schopf P, Behera SK, Carton J, Kessler WS, Meyers G, Qu T, Schott F, Shetye S, Xie SP (2006) Climate fluctuations of tropical coupled systems. The role of ocean dynamics. J Clim 19:5122–5174

Church J, Clark PU, Cazenave A, Gregory J, Jevrejeva S, Levermann A, Merrifield MA, Milne GA, Nerem RS, Nunn PD, Payne AJ, Pfeffer WT, Stammer D, Unnikrishnan AS (2013) Climate Change 2013: The Physical Science Basis. Contribution of Working Group I to the Fifth Assessment Report of the Intergovernmental Panel on Climate Change, Cambridge University Press, Cambridge, United Kingdom and New York, NY, USA, chap Sea Level Change

Church JA, White N (2011) Sea-level rise from the late 19th to the early 21st century. Surv Geophys 32:585–602

Coco G, Senechal N, Rejas A, Bryan K, Capo S, Parisot J, Brown J, MacMahan J (2014) Beach response to a sequence of extreme storms. Geomorphology 204:493–501

Dangendorf S, Rybski D, Mudersbach C, Mller A, Kaufmann E, Zorita E, Jensen J (2014) Evidence for long-term memory in sea level. Geophys Res Lett 41:5530–5537

Dasgupta S, Laplante B, Murray S, Wheeler D (2009) Climate change and the future impacts of storm surge disasters in developing countries. Technical Report, CGD Working Paper 182, Washington, D.C.: Center for Global Development. http://www.cgdev.org/content/publications/detail/1422836

Dean RG, Houston JR (2013) Recent sea level trends and accelerations: comparison of tide gauge and satellite results. Coast Eng 75:4–9

Dee D, Uppala SM, Simmons AJ, Berrisford P, Poli P, Kobayashi S, Andrae U, Balmaseda MA, Balsamo G, Bauer P, Bechtold P, Beljaars ACM (2011) The ERA-interim reanalysis: configuration and performance of the data assimilation system. Q J R Meteorol Soc 137:553–597

Goddard PB, Yin J, Griffies SM, Zhang S (2015) An extreme event of sea-level rise along the Northeast coast of North America in 2009–2010. Nat Commun 6:6346

Guedes R, Bryan K, Coco G, Holman R (2011) The effects of tides on swash statistics on an intermediate beach. J Geophys Res 116:C04,008

Guza R, Feddersen F (2012) Effect of wave frequency and directional spread on shoreline runup. Geophys Res Lett 39:L11,607

Hamlington BD, Strassburg M, Leben RR, Han W, Nerem RS, Kim KY (2014) Uncovering an anthropogenic sea-level rise signal in the Pacific Ocean. Nat Clim Chang 4(9):782–785

Hemer M, Wang X, Church J, Swail V (2010) Coordinated global ocean wave projections. Bull Am Meteorol Soc 91(4):451–454

Hemer MA, Fan Y, Mori N, Semedo A, Wang XL (2013) Projected future changes in wind-wave climate in a multi-model ensemble. Nat Clim Chang 3:471–476

Hoeke RK, McInnes KL, Kruger JC, McNaught RJ, Hunter JR, Smithers SG (2013) Widespread inundation of Pacific islands triggered by distant-source wind-waves. Glob Planet Chang 108:128–138

Holgate SJ (2007) On the decadal rates of sea level change during the twentieth century. Geophys Res Lett 34:L01,602

Holman R, Sallenger A (1985) Setup and swash on a natural beach. J Geophys Res 90(C1):945–953

Jevrejeva S, Moore JC, Grinsted A, Woodworth PL (2008) Recent global sea level acceleration started over 200 years ago? Geophys Res Lett 35:L08,715

Komar P (1998) Beach processes and sedimentation, 2nd edn. Prentice Hall, New Jersey, USA

Laibi R, Anthony E, Almar R, Castelle B, Senechal N (2014) Morphodynamic characterisation of the human-impacted Bight of Benin sand barrier coast, West Africa. J Coast Res Spec Issue 70:078–083

Laudier N, Thornton E, MacMahan J (2011) Measured and modeled wave overtopping on a natural beach. Coast Eng 58:815–825

Le Cozannet G, Cazenave A (2014) Approaches to evaluate the recent impacts of sea-level rise on shoreline changes. Earth-Sci Rev 138:47–60

Longuet-Higgins MS, Stewart RW (1962) Radiation stress and mass transport in gravity waves with application to "surf-beats". J Fluid Mech 8:565–583

Losada I, Reguero B, Mendez F, Castanedo S, Abascal A, Minguez R (2013) Long-term changes in sea-level components in Latin America and the Caribbean. Glob Planet Chang 104:34–50

Lyu K, Zhang X, Church JA, Slangen ABA, Hu J (2014) Time of emergence for regional sea-level change. Nat Clim Chang 4:1006–1010
Matias A, Williams J, Masselink G, Ferreira O (2012) Overwash threshold for gravel barriers. Coast Eng 63:48–61
Menendez M, Woodworth PL (2010) Changes in extreme high water levels based on a quasi-global tide-gauge data set. J Geophys Res 115:C10,011
Merrifield MA, Thompson PR, Lander M (2012) Multidecadal sea level anomalies and trends in the western tropical Pacific. Geophys Res Lett 39
Meyssignac B, Cazenave A (2012) Sea level: a review of present-day and recent-past changes and variability. J Geodyn 58:96–109
Meyssignac B, Becker M, Llovel W, Cazenave A (2012) An assessment of two-dimensional past sea level reconstructions over 1950-2009 based on tide gauge data and different input sea level grids. Surv Geophys 33:945–972
Mitchum GT, Nerem SR, Merrifield MA, Gehrels WR (2010) Understanding Sea Level Rise and Variability, Chapter Modern sea level changes estimates. In: Church J. A., Woolworth P. L., Aarup T., Wilson W. S. (eds). Wiley-Blackwell Publishing, London, UK
Nicholls RJ, Cazenave A (2010) Sea-level rise and its impact on coastal zones. Science 328:1517–1520
Palanisamy H, Cazenave A, Delcroix T, Meyssignac B (2015) Spatial trend patterns in the Pacific Ocean sea level during the altimetry era: the contribution of thermocline depth change and internal climate variability. Ocean Dyn 65:341–356
Passaro M, Cipollini P, Vignudelli S, Quartly GD, Snaith HM (2014) ALES: a multi-mission adaptive subwaveform retracker for coastal and open ocean altimetry. Remote Sens Environ 145:173–189
Piecuch CG, Ponte RM (2013) Buoyancy-driven interannual sea level changes in the tropical South Atlantic. J Phys Oceanogr 43:533–547
Plant N, Stockdon H (2015) How well can wave runup be predicted? Comment on Laudier et al (2011) and Stockdon et al (2006). Coast Eng 102:44–48
Ranasinghe R, Callaghan D, Stive MJF (2012) Estimating coastal recession due to sea level rise: beyond the bruun rule. Clim Chang 110:561–574
Ray RD, Douglas BC (2011) Experiments in reconstructing twentieth-century sea levels. Prog Oceanogr 91:496–515
Richter I, Xie SP, Behera SK, Doi T, Masumoto Y (2014) Equatorial Atlantic variability and its relation to mean state biases in CMIP5. Clim Dyn 42:171–188
Ruessink B (1998) The temporal and spatial variability of infragravity energy in a barred nearshore zone. Cont Shelf Res 18:585–605
Senechal N, Coco G, Bryan K, Holman R (2011) Wave runup during extreme storm conditions. J Geophys Res 116:C07,032
Serafin KA, Ruggiero P (2014) Simulating extreme total water levels using a time-dependent, extreme value approach. J Geophys Res 119:6305–6329
Stammer D, Cazenave A, Ponte RM, Tamisiea ME (2013) Annual Review of Marine Science, Vol. 5, Annual Reviews, Palo Alto, CA, USA, chap Causes for contemporary regional sea level changes
Stive MJF (2004) How important is global warming for coastal erosion? An editorial comment. Clim Chang 64:1–2
Stockdon HF, Holman RA (2000) Estimation of wave phase speed and nearshore bathymetry from video imagery. J Geophys Res 105(C9):22,015–22,033
Stockdon HF, Holman RA, Howd PA, Sallenger AH (2006) Empirical parameterization of setup, swash, and runup. Coast Eng 53:573–588
Symonds G, Huntley A, Bowen A (1982) Two-dimensional surf-beat: long-wave generation by a time-varying breakpoint. J Geophys Res 87:492–498
Tamisiea ME (2011) Ongoing glacial isostatic contributions to observations of sea level change. Geophys J Int 186:1036–1044
Timmermann A, McGregor S, Jin F (2010) Wind effects on past and future regional sea level trends in the southern Indo-Pacific. J Clim 23(16):4429–4437
Toualy E, Aman A, Koffi P, Marin F, Wango TE (2015) Ocean swell variability along the northern coast of the Gulf of Guinea. Afr J Mar Sci 37(3)
Vignudelli S, Kostianoy A, Cipollini P, Beneviste J (eds) (2011) Coastal Altimetry. Springer
Vinogradov SV, Ponte RM, Heimbach P, Wunsch C (2008) The mean seasonal cycle in sea level estimated from a data-constrained general circulation model. J Geophys Res 113:C03,032
Von Storch H, Zwiers F (1999) Statistical analysis in climate research. Cambridge University Press
Walton TLJ, Dean RG (2009) Landward limit of wind setup on beaches. Ocean Eng 36(9-10):763–766
Wolf J (2009) Coastal flooding: impacts of coupled wave-surge-tide models. Nat Hazards 49(2):241–260
Wong P, Losada IJ, Gattuso JP, Hinkel J, Khattabi A, McInnes KL, Saito Y, Sallenger A (2013) Coastal systems and low-lying areas. In: Climate Change 2014: Impacts, Adaptation, and Vulnerability. Part A: Global and Sectoral Aspects. Contribution of Working Group II to the Fifth Assessment Report of the Intergovernmental Panel on Climate Change. Cambridge University Press, Cambridge, United Kingdom and New York, NY, USA
Woodworth P, Gregory J, Nicholls R (2004) The Sea, Harvard University Press, Harvard, USA., chap Long term sea-level changes and their impacts, p Volume 13
Woppelmann G, Letetrel C, Santamaria A, Bouin MN, Collilieux X, Altamini Z, Williams SDP, MartinMiguez B (2009) Rates of sea-level change over the past century in a geocentric reference frame. Geophys Res Lett 36:L12,607
Wright LD, Short AD (1984) Morphodynamic variability of surf zones and beaches: a synthesis. Mar Geol 56:93–118
Wunsch C, Stammer D (1997) Atmospheric loading and the oceanic ”inverted barometer” effect. Rev Geophys 35:79–107